

## Atomic-Resolution Dynamic Force Microscopy and Spectroscopy of a Single-Walled Carbon Nanotube: Characterization of Interatomic van der Waals Forces

Makoto Ashino,\* Alexander Schwarz, Timo Behnke, and Roland Wiesendanger

*Institute of Applied Physics, University of Hamburg, Jungiusstrasse 11, D-20355 Hamburg, Germany*

(Received 2 April 2004; published 20 September 2004)

We report atomic-resolution imaging and site-specific quantitative force measurements on a single-walled carbon nanotube by dynamic force microscopy and three-dimensional force field spectroscopy at low temperatures. The topography imaged in the attractive force regime reflects the trigonal arrangement of the hollow sites as maxima. Individual force curves were unambiguously assigned to carbon atoms and hollow sites, respectively. Site-specific quantitative evaluation revealed that the short-range interatomic van der Waals forces are responsible for the atomic-scale contrast.

DOI: 10.1103/PhysRevLett.93.136101

PACS numbers: 68.37.Ps, 34.20.Cf, 61.46.+w

Dynamic force microscopy (DFM) has been extensively used for the investigation of sample surfaces regardless of their conductivity [1]. In this experimental setup, a cantilever with eigenfrequency  $f_0$  is oscillated at an amplitude  $A$  by a self-excitation resonance loop. Application of the frequency modulation technique in which surface imaging has been realized by detecting the frequency shift  $\Delta f$  due to tip-sample interactions has enabled significant improvements of imaging surfaces with nonperiodic features and point defects. So called “true” atomic-resolution has been achieved in the non-contact regime [2]. The distance dependence of the interaction forces  $F(z)$  can be determined in dynamic force spectroscopy (DFS) by recording either  $\Delta f(z)$  [3,4] or  $\Delta f(A)$  [5] curves at a given  $xy$  position and converting them into force data [3,6,7]. Recently, DFS was performed on specific atomic lattice sites [8]. Using three-dimensional force field spectroscopy (3D-FFS),  $F(x, y, z)$  data were obtained at every image point [9]. Thereby, it has become possible to assign individual curves unambiguously to specific atomic lattice sites [10].

In this Letter, we report true atomic-resolution DFM imaging in the noncontact regime on a single-walled carbon nanotube (SWNT) and by application of 3D-FFS successful quantification of short-range forces and adhesion energies above SWNT’s specific atomic lattice sites. We found that rather weak interatomic van der Waals (vdW) forces are responsible for the atomic-scale contrast. So far high-resolution imaging with high-precision force sensing has been limited to flat and relatively reactive surfaces [8–10]. The rather strong short-range chemical-bonding forces between the foremost tip atom and the surface atom underneath have been found to be on the order of 1 nN, in good agreement with theoretical predictions [11]. For the nonreactive flat surfaces, true atomic-resolution imaging and respective computer simulations on graphite(0001) [4] and Xe(111) [12] indicated that the weak short-range vdW forces should be dominant. However, experimental site-specific DFS data to support this claim has not been available up to now.

The SWNT consists of a “single” graphene sheet rolled up into a seamless cylinder with diameter below 2 nm and length up to hundreds of  $\mu\text{m}$ . Within the graphene sheet, carbon (C) atoms are located at the corners of regular arranged hexagonal aromatic rings, whose centers are the trigonally arranged hollow (H-) sites of the honeycomb structure. The SWNTs tend to form close packed bundles due to the nonbonding vdW interaction [13]. Physi- and chemisorption and nonbonding and bonding sidewall functionalization have attracted increasing attention for application to gas sensors [14], doping of SWNT-based electronic devices [15], biosensors [16], and so on. Recently, the interaction with water and DNA molecules has been investigated [17–19]. Computer simulation indicated that the vdW forces should be dominant for DNA encapsulation into SWNTs [19].

The 3D-FFS with atomic-scale spatial resolution revealed the 3D force fields specifically dependent on the C and H sites of a SWNT’s cylindrical honeycomb layer. These results are of profound significance because SWNTs are not only promising materials for the nano-scale functionalization but also, due to their quasi-one-dimensional structure with chiralities and high transversal flexibilities, well-defined model systems of curved soft materials including biological macromolecules with helical structure. The ability to detect the rather weak vdW forces is indispensable to examine interfaces with organic systems on the atomic scale. Therefore, the achievement of site-specific quantification of the interatomic vdW forces can stimulate investigations of soft, curved and weakly interacting materials.

The experiments were performed with our home-built ultrahigh vacuum low-temperature force microscope optimized for atomic-scale studies [20]. Background pressure and temperature were  $p < 1 \times 10^{-8}$  Pa and  $T = 11$  K, respectively. All results were acquired using a silicon (Si) cantilever with a very sharp tip of nominal radius (given by the manufacturer)  $R_{\text{nom}} = 2$  nm [21]. The spring constant and the resonance frequency of the cantilever were  $c_z = 34.3$  N/m and  $f_0 = 159$  kHz, re-

spectively. The tip was *in situ* cleaned by argon ion sputtering ( $t = 4$  min,  $U_{\text{ex}} = 620$  eV, and  $I_{\text{ion}} = 4$  mA). During measurement, the cantilever was operated in the constant amplitude mode. To cancel the electrostatic forces, the average contact potential difference was compensated by applying a bias voltage  $U_{\text{bias}} = -0.31$  V to the cantilever (sample: grounded). The SWNTs with a typical diameter  $d = 1.38$  nm [22] were deposited from a 1,2-dichloroethane dispersion on an air-cleaved graphite. After transfer into ultrahigh vacuum, the sample was heated at  $300^\circ\text{C}$  for 1.5 hours to remove contaminations.

The 3D view in Fig. 1 demonstrates that atomic resolution has been achieved on the curved surface of an individual SWNT. By comparing with low magnification images, the SWNT was found to be in a bundle, which runs parallel to the  $y$  direction. The atomic-scale contrast, obtained for other SWNTs in the bundle as well, is strong in an approximately  $0.6$  nm-wide top region but becomes blurry towards the sloping sides. In general, the atomic-scale contrast can be realized by the short-range forces acting between the foremost tip atom and the sample atom directly below. For geometrical reasons, more atoms can be involved in the short-range forces on the sloping sides. The additivity of the multiple interatomic forces may reduce the atomic-scale contrast.

Figure 2(a) shows a close-up image in top view acquired around the center of Fig. 1. Each topographic maximum has six nearest neighbors separated by about  $250$  pm parallel and  $280$  pm perpendicular to the tube axis. Lattice distortions might be related to the specific atomic structure of the tip apex. However, elongations of separations perpendicular to the nanotube axis can be explained geometrically by assuming a pointlike tip scanning across a curved surface [23]. Taking this into ac-

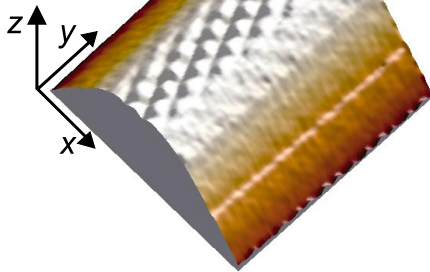


FIG. 1 (color). A three-dimensional view of the atomically-resolved carbon nanotube image acquired under constant frequency shift feedback control in the noncontact regime;  $\Delta f = -65.3$  Hz,  $A = 2.4$  nm, image size  $3$  nm  $\times$   $3$  nm. The atomic-scale features are clearly observed around the elevated topmost area and are still slightly observed on the sloping sides. The maximum corrugation amplitude is about  $40$  pm.

count, from the observed symmetry and the undistorted separation along the nanotube axis we infer that the H sites are imaged as topographic maxima. This agrees well with the atomic-scale contrast on graphite(0001) acquired in the noncontact regime, where the comparison with simulations indicates that the H sites are imaged as topographic maxima. Note that the AB stacking of hexagonal graphite results in two inequivalent C ( $C_A$  and  $C_B$ ) sites [4]. Obviously, this can be ruled out for the SWNT, consisting of a single atomic layer. Therefore, the assignment of the maxima to the H sites is unambiguous. Furthermore, from comparison with the distinguishable topographic minima observed on the graphite(0001), we expect that the equivalent C sites of the SWNT are imaged as the indistinguishable minima in Fig. 2(a).

To determine the force versus distance relationships above specific atomic sites of the SWNT, we captured a full 3D force field with  $20 \times 20 \times 512$  data points in a box of nominally  $1$  nm  $\times$   $1$  nm  $\times$   $3$  nm above the same scan area as Fig. 2(a). The data acquisition was performed as described in Ref. [9,10]. First, the tip was stabilized at  $\Delta f_{\text{stab}} = -69.6$  Hz and then, after switching off the  $z$  feedback, approached by  $11.5$  pm toward the sample. The  $\Delta f(z)$  data was recorded during tip retraction by  $3$  nm and again during approach by  $3$  nm. After reestablishing  $z$  regulation, the tip was moved to the next  $xy$ -position, and the procedure was repeated. The total acquisition time was  $65$  min. In addition,  $\Delta f(z)$  data of  $512$  points were recorded during retraction and approach by  $12$  nm at several positions in the same scan area to characterize the forces in the long-range regime.

Figure 2(b) displays the  $z$  values recorded at the stabilization points, which show no significant drift, but trace

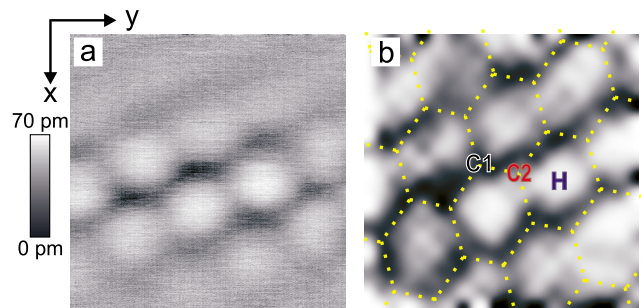


FIG. 2 (color). (a) Constant frequency shift image with atomic-scale features;  $\Delta f = -69.6$  Hz,  $A = 2.3$  nm, image size  $1$  nm  $\times$   $1$  nm. For better visualization of the atomic-scale features, a parabolic curvature has been subtracted from the raw data. (b) Contour plot of the  $z$  values recorded at the stabilizing points during capturing the 3D-FFS. Note that the  $20 \times 20$  data points have been extrapolated to  $400 \times 400$  image points for better visualization. The individual  $\Delta f(z)$  curves acquired at the positions labeled C1, C2, and H are shown in Fig. 3. The slightly distorted corresponding carbon lattice is depicted on the image.

nearly perfectly the contour lines of the topographic image shown in Fig. 2(a). Particularly, the atomic structure can be directly identified, whereby the assignment of individual spectroscopy curves to specific atomic lattice sites is unambiguously possible. Each  $\Delta f(z)$  curve was converted into force data set, i.e.,  $F(z)$  curve, using the potential deconvolution method [6,24]. Note that this method works, in principle, for the whole range of the interaction forces but is suited best for the range which are small compared to the amplitude  $A$  [6,7,24].

The analysis of three typical individual curves is shown in Fig. 3. All were acquired during retraction. No obvious difference, i.e., no hysteresis corresponding to

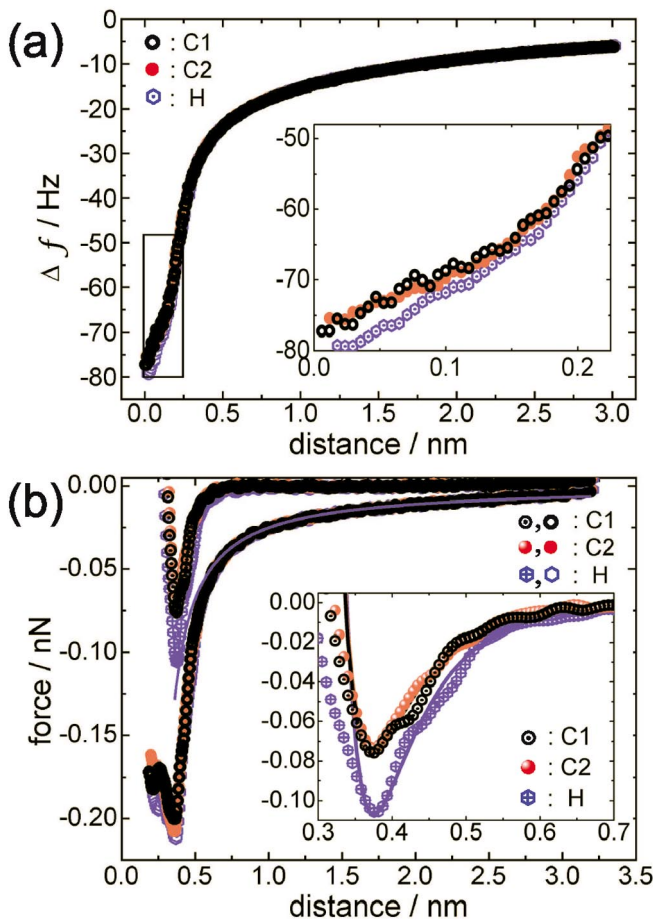


FIG. 3 (color). Analysis of individual spectroscopy curves above the specific atomic sites of the hexagonal carbon lattice. (a)  $\Delta f(z)$  curves measured above the positions C1, C2, and H in Fig. 2(b). The close proximity regime is magnified in the inset. (b) The total interaction forces  $F(z)$  (lower curves) have been directly converted from  $\Delta f(z)$  curves in (a). The blue line has been fitted to the long-range force data from 3.2 to 1 nm using a  $1/z$  force law. The short-range forces  $F_{\text{short}}$  (upper curves) are obtained by subtracting the long-range fit from the total forces. The inset displays the close proximity regime (symbols) together with the corresponding L-J force fits (lines). The starting points were adjusted for the L-J fittings.

energy dissipation, was observed between the curves for retraction and approach. Thereby all procedures can be regarded as reversible. The curves have been recorded above the neighboring carbon atoms C1 (black) and C2 (red) and the hollow site H (blue). The  $\Delta f(z)$ -plots are shown in Fig. 3(a). The starting points were adjusted to reflect the different  $z$  values of the regulating points, and the zero point was arbitrarily set to the closest approach. For distances  $z = 3$  to 0.2 nm, the curves are nearly indistinguishable as expected for long-range forces. In contrast, the close proximity regime in the inset, where the short-range forces dominate, shows that the slopes of the curves C1 and C2 become gentler from about 0.18 nm than the curve H. At the regulating point of  $\Delta f = -69.6$  Hz, the horizontal difference between the curves C1 and H is about 42 pm, corresponding to the corrugation between the topographic maximum and minimum in Fig. 2(a). On the other hand, the difference between the neighboring two C sites is negligibly small as expected for SWNT because all atoms should be equivalent.

The total interaction forces  $F(z)$  derived from the  $\Delta f(z)$  data are plotted in Fig. 3(b) for the sites C1, C2, and H. The attractive forces at their specific sites attain the maximal values  $F_{\text{total}}^{\text{max}} \approx -200$ ,  $-208$ , and  $-212$  pN, respectively. Previously, maximal values of about  $-8.6$  nN [5] and  $-6.7$  nN [24] have been reported without any site specifications on the graphite(0001). The large difference can be explained by the magnitude of the long-range background forces. The Si tips with larger nominal radius  $R_{\text{nom.}} = 10$  nm [25] used in Refs. [5,24] generally result in larger long-range vdW interaction. Furthermore, despite the identical chemical composition of SWNTs and graphite, the much lower density in the  $z$  direction of the hollow SWNTs compared with the layered graphite reduces the Hamaker constant and leads to a smaller long-range vdW interaction.

In the close proximity regime, short-range forces  $F_{\text{short}}$  become dominant. To determine the  $F_{\text{short}}$ , we apply the same procedure as described in Ref. [10]. First, we approximated the long-range forces  $F_{\text{long}}$  by  $F_{\text{long}}(z) = \frac{B}{z+z_1}$ , where  $B$  and  $z_1$  are fitting parameters [26]. The constant  $B$  with energy unit indicates the magnitude of the long-range forces. The offset  $z_1$  is utilized to adjust the  $z$  coordinate since the starting point of each curve was based on the regulating point. Next, to obtain reliable fits for the long-range parts, the data recorded at distances up to 12 nm were examined. By setting  $B = -125$  meV, we find excellent agreement with the experimental data. In succession, by fixing  $B$  and changing  $z_1$ , excellent fits were found with  $z_1 = -0.020$  nm,  $-0.020$  nm and  $+0.020$  nm for the curves C1, C2, and H, respectively. By comparing the  $\Delta f_{\text{re}}(z)$  recalculated using the obtained  $B$  [27] with our data, the validity of the potential deconvolution method for the long-range regime were confirmed. In contrast to  $B = -850$  meV in

Ref. [10], where a tip with a larger nominal radius [25] was used and the electrostatic forces were not minimized, the obtained  $B = -125$  meV in our experiments indicates a much smaller long-range contribution.

By subtracting the long-range fit from the total force, the short-range force is obtained;  $F_{\text{short}}(z) = F_{\text{total}}(z) - F_{\text{long}}(z)$ . In the inset of Fig. 3(b), the difference between the  $F_{\text{short}}(z)$  curves for the neighboring carbon atoms labeled C1 and C2 is negligibly small, as expected for indistinguishable carbon atoms, comparing with the curve for the H-site. The attractive short-range forces attain the maximal values  $F_{\text{short}}^{\text{max}} = -75.8$ ,  $-73.4$ , and  $-106$  pN (contribution to the maximal total forces  $F_{\text{total}}^{\text{max}}$ : 37.9%, 35.3%, and 50.0%) for C1, C2, and H, respectively [28]. On the other hand, the short-range chemical-bonding forces on NiO(001) are about 0.7 nN and 1.1 nN (contribution to the total force: about 71% and 82%) for the atomic maximum and minimum, respectively [9,10]. Comparing with the chemical-bonding forces, the acquired values of the  $F_{\text{short}}^{\text{max}}$  and their contribution to the total forces are very small. Nevertheless, the differences between  $F_{\text{short}}^{\text{max}}$  for the H site and for the C1 and C2 sites are relatively large. These results indicate that indeed interatomic short-range vdW forces were successfully utilized to achieve atomic-scale contrast.

For further analysis of  $F_{\text{short}}$ , we compared our data with the short-range force derived from a simple Lennard-Jones (L-J) pair potential as in Refs. [4,24]. By fixing the equilibrium distance as 0.334 nm and taking the binding energy  $E_0$  as fitting parameter, we find excellent fits, particularly from far to the distance  $z_{\text{max}}$  exhibiting  $F_{\text{short}}^{\text{max}}$ , attaining  $E_0 = 58.9$ ,  $57.0$ , and  $82.7$  meV for the curves C1, C2, and H, respectively [28]. Note that the potential deconvolution method to derive  $F(z)$  from  $\Delta f(z)$  [6] is strictly valid for the proximate regime. The obtained  $E_0$  values are on the same order as the adhesive energy of a water monomer on the SWNT [17]. Therefore, the  $F_{\text{short}}(z)$  can be regarded as the interatomic vdW forces dominating in molecular physisorption despite unsaturated chemical-bonding character of the foremost Si tip atom. The deviations of the experimental data from a L-J fit at  $z < z_{\text{max}}$ , where the repulsive term becomes prominent, might be related to the transversal flexibilities of the hollow tube in contrast to the rigid Si tip [29].

In conclusion, we for the first time achieved atomic resolution on the soft curved surface of a SWNT by DFM. Using 3D-FFS, we successfully quantified the distance dependency of the short-range interatomic vdW forces above the specific atomic lattice sites and proved that indeed short-range interatomic vdW forces are responsible for atomic-scale contrast.

We appreciate C. Dekker, S. G. Lemay, H. Hölscher, and T. Maltezopoulos for fruitful discussions. Financial support from the EU project “NANOSPECTRA” and the DFG Graduate School “Design and characterization of

functional materials” is gratefully acknowledged.

\*To whom correspondence should be addressed. Electronic address: mashino@physnet.uni-hamburg.de

- [1] S. Morita, R. Wiesendanger, and E. Meyer, *Noncontact Atomic Force Microscopy* (Springer, New York, 2002).
- [2] F. J. Giessibl, *Science* **267**, 68 (1995).
- [3] B. Gotsmann and H. Fuchs, *Phys. Rev. Lett.* **86**, 2597 (2001).
- [4] H. Hölscher *et al.*, *Phys. Rev. B* **62**, 6967 (2000).
- [5] H. Hölscher *et al.*, *Phys. Rev. Lett.* **83**, 4780 (1999).
- [6] U. Dürig, *Appl. Phys. Lett.* **76**, 1203 (2000).
- [7] F. J. Giessibl, *Appl. Phys. Lett.* **78**, 123 (2001).
- [8] M. A. Lantz *et al.*, *Science* **291**, 2580 (2001).
- [9] H. Hölscher *et al.*, *Appl. Phys. Lett.* **81**, 4428 (2002).
- [10] S. M. Langkat, *Surf. Sci.* **527**, 12 (2003).
- [11] R. Pérez *et al.*, *Phys. Rev. B* **58**, 10835 (1998).
- [12] W. Allers *et al.*, *Europhys. Lett.* **48**, 276 (1999).
- [13] R. Saito, G. Dresselhaus, and M. S. Dresselhaus, *Physical Properties of Carbon Nanotubes* (Imperial College Press, London, 1998).
- [14] J. Kong *et al.*, *Science* **287**, 2000 (2000).
- [15] S. J. Tans, A. R. M. Verschueren, and C. Dekker, *Nature (London)* **393**, 49 (1998).
- [16] K. A. Williams *et al.*, *Nature (London)* **420**, 761 (2002).
- [17] T. Werder *et al.*, *J. Phys. Chem. B* **107**, 1345 (2003).
- [18] G. Hummer, J. C. Rasiah, and J. P. Noworyta, *Nature (London)* **414**, 188 (2001).
- [19] H. Gao *et al.*, *Nano Lett.* **3**, 471 (2003).
- [20] W. Allers *et al.*, *Rev. Sci. Instrum.* **69**, 221 (1998).
- [21] Silicon Cantilever SSS-NCL, Nanosensors, Switzerland.
- [22] A. Thess *et al.*, *Science* **273**, 483 (1996).
- [23] V. Meunier and P. Lambin, *Phys. Rev. Lett.* **81**, 5588 (1998).
- [24] H. Hölscher *et al.*, *Phys. Rev. B* **61**, 12678 (2000).
- [25] Silicon Cantilever NCL, Nanosensors, Switzerland.
- [26] Such a  $1/z$ -force law describes the quite plausible assumption of a vdW force between a cone or pyramid (tip) and a plane (graphite) and cylinders (SWNTs). Here we choose it to directly compare our results with Ref. [10]. More elaborate analytical models are available and can be in principle employed to estimate the tip radius. Using a model: sphere above cylinders on plane and  $H = 0.175$  aJ, we found  $R = 2.5$  nm. Considering that  $H$  is not precisely known but only reasonable guess, this result is in good agreement with  $R_{\text{nom.}} = 2$  nm.
- [27] H. Hölscher, U. D. Schwarz, and R. Wiesendanger, *Appl. Surf. Sci.* **140**, 344 (1999).
- [28] By comparing with the values for other atomic lattice sites within the topmost area showing the clearest atomic-scale contrast, the standard deviations are found to be about  $\pm 2.5$  pN for  $F_{\text{short}}^{\text{max}}$  and  $\pm 1.7$  meV for  $E_0$ , respectively. As discussed in Ref. [10], however, the estimated systematic error is about 30% in our experimental system.
- [29] According to increase of the repulsive term, radial deformation of the SWNT, which can make the repulsive contribution weaker than the  $(1/z)^{13}$  law, might occur.